Cross sections for the ^{7}Li(d,p)^{8}Li, ^{6}Li(^{3}He,n)^{8}B, ^{6}Li(d,α)^{4}He, ^{6}Li(d,p)^{7}Li, and ^{6}Li(d,n)^{7}Be reactions

Charles R. McClenahan* and Ralph E. Segel
Northwestern University, Evanston, Illinois 60201†
and Argonne National Laboratory, Argonne, Illinois 60439‡
(Received 19 August 1974)

The ^{7}Li(d, p)^{8}Li, ^{6}Li(^{3}He, n)^{8}B, ^{6}Li(d, α)^{4}He, ^{6}Li(d, p)^{7}Li, and ^{6}Li(d, n)^{7}Be reactions have been studied, chiefly at bombarding energies below 3.8 MeV. All five of these reactions have potential applications in controlled thermonuclear systems. Total cross sections, believed to be accurate to 15%, which is sufficient for reactor design, have been determined in all cases. Residual activity was counted in the ^{7}Li(d, p) and ^{6}Li(^{3}He, n) studies while the yield of the ^{7}Be 428-keV γ ray was measured in the ^{6}Li(d, n) investigation. Extensive angular distribution measurements were made for the ^{6}Li(d, α) and ^{6}Li(d, p) reactions and some discussion is given of the reaction mechanisms. Wherever possible, detailed comparisons are given to previously reported results.

[NUCLEAR REACTIONS ^{7}Li(d, p), E = thresh. −3.8 MeV; measured $\sigma(E)$; ^{6}Li(^{3}He, n), E = thresh. −7.5 MeV measured $\sigma(E)$; ^{6}Li(d, α), E = 0.5–3.4 MeV, measured $\sigma(E, \theta)$; ^{6}Li(d, p), E = 0.5–3.4 MeV measured $\sigma(E, \theta)$; ^{6}Li(d, n), E = 0.5–3.4 MeV, measured 0.428 MeV γ, deduced $\sigma(E)$.]

I. INTRODUCTION

A. Motivation

The expanding interest in the development of controlled thermonuclear reactors has led to the need to know the total cross sections of a variety of reactions involving light nuclei. While the major efforts in controlled thermonuclear research continue to be concentrated on reactors fueled by the ^{2}H(d, n)^{3}He or ^{2}H(t, n)^{4}He reactions, whose cross sections are quite well known, the many difficulties being encountered in the attempt to design such reactors renders it prudent to examine other approaches. In particular, it is possible that other exoergic reactions among light nuclei can be utilized.

McNally[1] has suggested that ^{6}Li may be burned. Several energy producing chain reactions are possible, for example:

$$^6\mathrm{Li} + \alpha \rightarrow {}^6\mathrm{Li}^* + \alpha \quad Q = -2.184 \text{ MeV}$$

$$^6\mathrm{Li}^* \rightarrow \alpha + d \quad Q = 0.712 \text{ MeV}$$

$$d + {}^6\mathrm{Li} \rightarrow \alpha + \alpha \quad Q = 22.375 \text{ MeV}$$

$$\text{Net} \quad 2\,{}^6\mathrm{Li} \rightarrow 3\alpha \quad Q = 20.903 \text{ MeV}.$$

It is obvious that the relevant nuclear reaction cross sections must be known before the utility of a chain like the one above can be assessed; a knowledge of the cross sections to an accuracy of 25% appears to be sufficient for reactor design purposes.[2] However, in attempting to assess the viability of various schemes it has become apparent that much of the necessary nuclear data is absent.[1-3]

Responding to these needs, the present work reports total cross-section measurements for several of the reactions of interest. Although some cross-section measurements have been previously reported for most of these reactions, the data are often fragmentary and, worse, frequently exhibit discrepancies between the measurements of different groups. In the present work stress has been placed on reliability, and it is felt that the errors in the quoted cross sections are less than the 25% that reactor-design considerations will permit.

In order to encourage the obtaining of the data most needed in controlled thermonuclear research (CTR) priority criteria have been proposed.[4] The highest priority (I) "shall be assigned to those nuclear data upon which some important aspect of CTR is immediately contingent." Table I lists the reactions that were studied in the present work and give the priority that they have been assigned. Three of the five are priority I.

B. Experimental procedures

Beams of deuterons and ^{3}He particles were accelerated by various accelerators at Argonne National Laboratory. Metallic lithium and LiF targets were used. Where residual activity was measured, the targets were LiF evaporated onto thick copper backings. When prompt spectra were taken, the targets were evaporated onto ≈30-μg/

cm^2 carbon backings. The Li metal targets were transferred into the chamber in vacuuo. The targets used for the ^{6}Li reactions were enriched to 99.3% ^{6}Li.

Two different methods were used to measure the target thicknesses. The energy loss in the LiF targets was determined by measuring the $^{19}F(p,\alpha\gamma)$ yield as a function of bombarding energy over an energy region where this reaction is known to be dominated by a single, narrow resonance. The resonance that was used most often is that at 872 keV. Rutherford scattering was used to measure the thickness of ^{6}Li metal targets. The yield of 2-MeV α particles scattered from the ^{6}Li was measured at several angles in order to verify that Rutherford scattering was dominant. The α particles scattered from the lithium could be resolved from those scattered from the carbon backing at angles equal to or larger than 40°. As a check on the agreement between these two methods, two ^{6}LiF targets were measured in both ways. The resonance technique gave the thicknesses 85 and 91 $\mu g/cm^2$, and alpha scattering gave 79 and 86 $\mu g/cm^2$, respectively. The results obtained with these two techniques differed by about 6%, which is well within the estimated uncertainty of the target thickness measurements. The thickness of all the LiF targets was taken to be that determined by the resonance technique, and the thickness of the Li metal targets was taken to be that determined by Rutherford scattering. In order to check the target thickness measurements further, 3-MeV protons were scattered from a weighed gold foil. The thickness as determined by Rutherford scattering agreed to within 0.5% with that determined by weighing. Unless otherwise stated, all of the targets used in the present work were in the 50–100-$\mu g/cm^2$ range.

Stability of the targets was checked by repeating points at the end of the target's use that were run at the beginning of the target's use. In some cases, thickness measurements were also made both before and after a target's use. In all cases the target was found to be stable to within the statistical uncertainty of the measurements, which varied from 1 to 5%.

If carbon builds up on the face of a target, then the bombarding particles will lose some energy before they reach the target, and the apparent energy of a resonance will shift. Therefore, measuring the target's thickness utilizing $^{19}F+p$ resonances after the target was used also gave a measure of the carbon buildup. Some carbon did build up, and therefore where the cross section was changing rapidly with energy the targets were changed frequently.

Two target chambers were used during the course of this work. When residual activity was measured, a chamber about 20 cm in diameter made of stainless steel was used. There was a 0.025-cm thick 3.8-cm diam steel window on the side of the chamber through which β rays could emerge and be counted by a scintillation detector. Also, a rotating can could be placed inside the chamber (Fig. 1). A sheet of cellulose nitrate plastic was wrapped inside the can to detect delayed α particles from the decay of the daughter nuclei. The entire chamber was insulated so that all of the charge entering the chamber could be integrated. The beam was pulsed, and the activity was detected while the beam was off.

When prompt reaction products were detected, a 76-cm diam standard scattering chamber which was built for use with surface barrier detectors was used. The chamber body was grounded, and the Faraday cup was insulated from, and attached to, the back of the chamber (Fig. 2). Reaction products were detected by surface barrier detectors that were thick enough to completely stop the protons from the $^{6}Li(d,p)^{7}Li$ reaction within their active volume. Two of the detectors were mounted on movable arms inside the chamber, and as many as three others were mounted in fixed positions. About eight runs were taken at each energy with the movable arms moved between runs such that the entire angular range was covered. The number of reaction products detected in each of the fixed counters was constant from run to run to within the statistical uncertainties. On the side of the chamber there was a 1-cm thick Lucite window

TABLE I. The reactions studied and reported in the present work.

Reaction	Priority	Q or threshold [a]	Energy range studied
$^{7}Li(d,p)^{8}Li$	4	$E_{th}=248$ keV	280 keV–3.8 MeV
$^{6}Li(^{3}He,n)^{8}B$	3	$E_{th}=2.966$ MeV	2.98 MeV–7.5 MeV
$^{6}Li(d,\alpha)^{4}He$	1	$Q=22.4$ MeV	500 keV–3.4 MeV
$^{6}Li(d,p)^{7}Li$	1	$Q=5.0$ MeV	500 keV–3.4 MeV
$^{6}Li(d,n_1)^{7}Be^*$	1	$Q=2.9$ MeV	500 keV–3 MeV

[a] Reference 5.

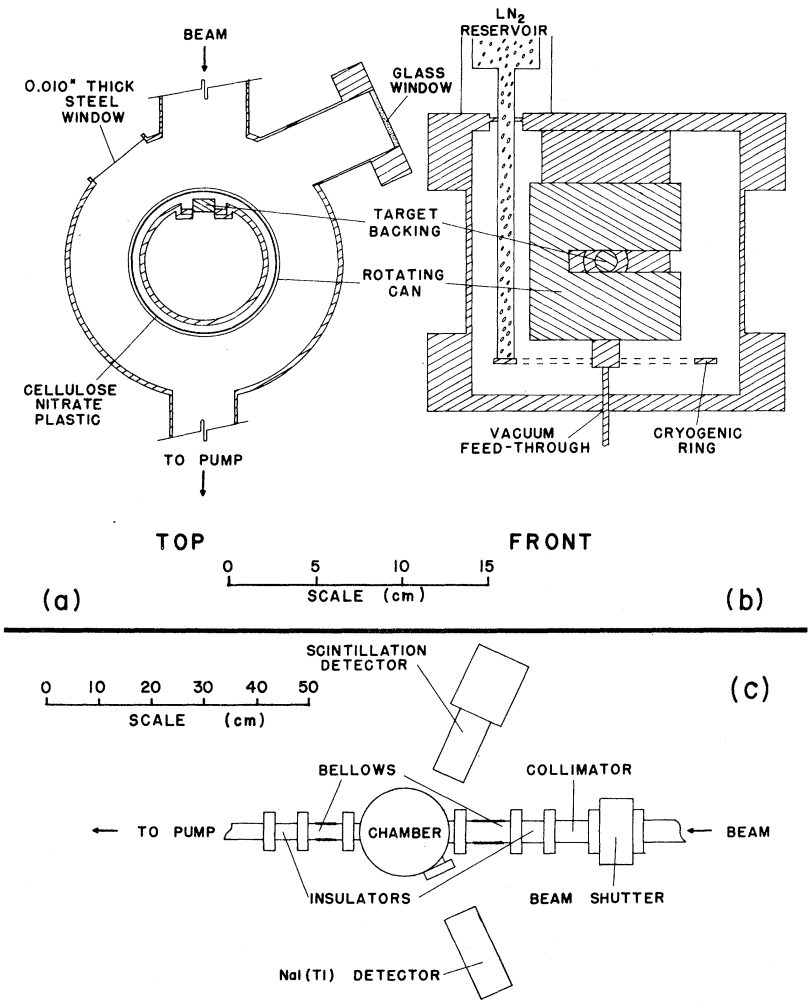

FIG. 1. The chamber that was used with both the cellulose nitrate plastic track detectors and the scintillation detectors to measure cross sections for the ^{7}Li$(d, p)^{8}$Li and ^{6}Li$(^{3}$He$, n)^{8}$B reactions by detecting the activity of the daughter nuclei. (a) Top view, (b) front view, (c) top view of chamber and beam line.

through which γ rays were detected.

A Brookhaven Instrument Corporation model 1000 current integrator was used to measure the integrated charge; it is guaranteed to be stable to 0.01% over several years and always accurate to within 0.1%.

To check for secondary electron emission from the target, a repelling voltage was applied to an insulated collimator which was in front of the 20-cm diam chamber. To within a 5% statistical accuracy the reaction product yields per unit integrated charge were found to be independent of repelling potential up to the maximum voltage tried (-1000 V). Moreover, there was no systematic relation between the repelling potential and the measured yields.

The fact that the thickness of a gold target as measured by Rutherford scattering agreed with the determination of the same quantity by weighing indicates that the charge integration in the 76-cm chamber was accurate. In addition, checks were made that the targets did not scatter a significant portion of the beam out of the Faraday cup. Only at beam energies below 1 MeV was beam scattering ever detectable and here targets sufficiently thin that they scattered out but a negligible fraction of the beam were used. Equality of the target-in and target-out currents was taken to indicate that the target was thin enough so that a significant portion of the beam was not scattered out of the Faraday cup. The current meter on the integrator could be read to an accuracy of about 5%.

The current integration and target thickness measurements were checked in a variety of ways,

and from these checks it is concluded that the target thickness uncertainty was no greater than 10%, and the error in the current integration in both chambers no more than 5%. These constitute the major uncertainties in the absolute cross-section measurements. The uncertainty of the detector efficiencies is felt to be, in all cases, less than 5%. Therefore, it is concluded that the over-all uncertainty in the absolute cross sections reported here is no more than 15%.

II. ^{7}Li$(d,p)^8$Li

This reaction is endoergic, $Q = -0.192$ MeV. (Unless otherwise noted, all energy level data are from Ref. 4.) Lithium-8 decays with a 0.85-sec half-life to the broad first excited state of ^{8}Be centered at 2.90 MeV, which, in turn, promptly decays into two α particles. Only the ground state and the 0.98-MeV first excited state of ^{8}Li are bound. The lab thresholds for the (d,p) reactions feeding these two states are 0.248 and 1.50 MeV, respectively.

Several groups have measured the β activity of ^{8}Li in order to determine the cross section for this reaction.[6-8] Baggett and Bame[6] report the cross section to be about a factor of 2 higher than that reported by Bashkin,[7] and Kavanagh[8] reports the cross section to be about 25% higher than does Bashkin. Of course, none of these measurements could distinguish between the (d,p_0) and (d,p_1) reactions. Chase *et al.*[9] have measured the yield of first excited-state γ rays. Sellschop[10] took angular distributions for the (d,p_0) reaction at six energies between 1.0 and 2.5 MeV.

In the present work, the residual ^{8}Li activity was detected. Therefore, at bombarding energies above 1.5 MeV, the present results include contributions from both the (d,p_0) and (d,p_1) reactions.

Two different types of detectors were employed. At deuteron energies above 500 keV, β spectra were taken by a 5-cm diam by 7.5-cm thick pilot B plastic scintillator. The beam from the Argonne Dynamitron was pulsed by electrostatic deflection plates, and the data were collected between beam bursts. Spectra were stored in the external memory of an ASI 2100 computer. The data were stored in a two-dimensional array of time after bombardment versus β energy.

Below 500 keV, deuterons were accelerated by a 2-MeV Van de Graaff accelerator. Tracks in a sheet of cellulose nitrate plastic (CN) of delayed α particles from the ^{8}Li decay were counted. This detector is insensitive to electrons. The CN, located inside a can in the chamber, rotated around the target subtending a nearly 2π solid angle (Fig. 1). The beam was pulsed by an upstream shutter, which was synchronized to the rotating can. At bombarding energies below 320 keV, targets which completely stopped the incident deuterons were used while above this energy the targets were, as usual, ~80 μg/cm^2 thick.

In the cases of both types of detector, decay curves were fitted to the data. These curves consisted of an exponential decay with the half-life of ^{8}Li plus a background. The chief background in the scintillator spectra was from the decay of ^{20}F, produced by the ^{19}F$(d,p)^{16}$O reaction in the target. Background in the scintillator spectra increased as the bombarding energy increased, reaching

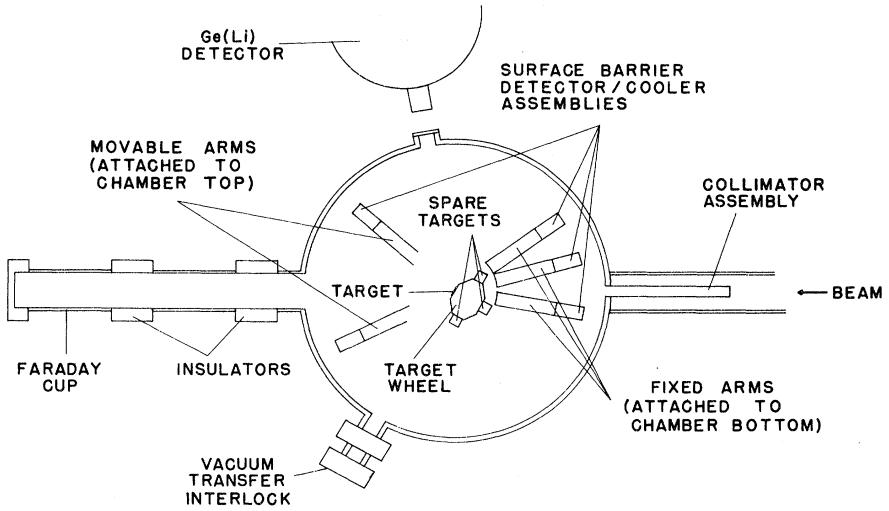

FIG. 2. A top view of the 76.2 cm diam scattering chamber that was used to measure the cross sections for the ^{6}Li$(d,p)^7$Li, ^{6}Li$(d,n)^7$Be*, and ^{6}Li$(d,\alpha)^4$He reactions.

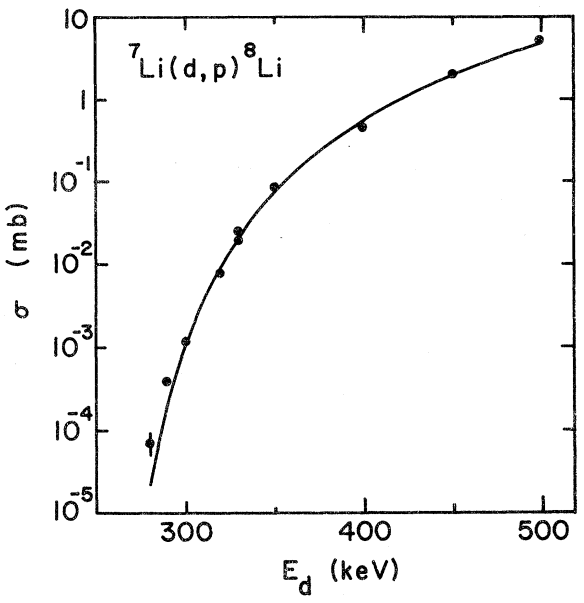

FIG. 3. Low-energy reaction cross section versus energy for the ^{7}Li(d, p)^{8}Li reaction. Cellulose-nitrate plastic track detectors were used in collecting these data. The solid curve represents a DWBA calculation of the yield curve.

about 50% of the initial decay rate when the bombarding energy was 3.8 MeV. The assumption of a constant track density background was found to be satisfactory for the CN data. Only at the lowest deuteron energies was the background in the CN significant. The lowest cross section reported here is 71 nb at 280 keV. Background, which was probably due to (n, α) reactions in the CN, prevented lower cross section from being measured. In situations where fast neutrons are not produced, the sensitivity of this technique could be increased by several orders of magnitude.

Figure 3 shows the cross section for the ^{7}Li-(d,p)^{8}Li reaction below 500 keV. Because of the Coulomb barrier, the cross section decreases rapidly with decreasing energy. In determining the cross section at the deuteron beam energy the reaction cross section was assumed to be proportional to the Coulomb penetrability of the outgoing proton which decreased as the deuterons lost energy in traversing the target. The cross section data shown on Fig. 3 are reported at the incident deuteron energy.

Since below 500 keV the energy dependence of the cross section for this reaction is determined chiefly by extranuclear terms, a distorted-wave Born-approximation (DWBA) calculation in which Coulomb and centrifugal barrier effects are properly included should do a good job of predicting this dependence. The data shown in Fig. 3 were compared with total cross sections calculated by the code DWUCK.[11] Optical-model parameters were taken from Refs. 12 and 13. The calculated curve is the solid line shown in Fig. 3. Different inner cutoff radii were tried and it was found that varying the inner cutoff radius from 0 to 7 fm produced less than a 20% change in the total cross section

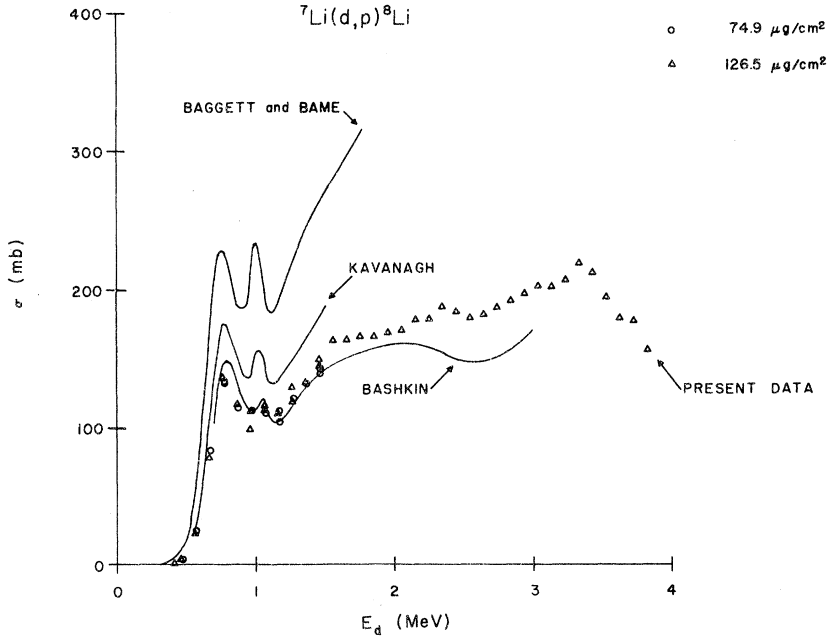

FIG. 4. Total cross section versus energy for the ^{7}Li(d, p)^{8}Li reaction. Also plotted are data from Refs. 5–7.

and therefore no inner cutoff radius was used in calculating the solid line of Fig, 2. As the inner cutoff radius was increased above 7 fm the calculated total cross section fell rapidly decreasing to 20% of the no cutoff value when the cutoff reached 13 fm.

There is a narrow resonance at 360 keV,[14] which was not studied here and does not show in the data presented here. No data points were taken where deuterons in the target were near to this resonance energy.

Results above 500 keV are shown in Fig. 4. Points below 500 keV would be indistinguishable from zero on the scale of Fig. 4 and are therefore omitted. At bombarding energies greater than 500 keV the variation of cross section with energy through the target could be neglected, and the cross sections are reported at the deuteron energy at the center of the target.

The solid curves in Fig. 4 represent the data reported in Refs. 6–8. The present data agree well with those of Bashkin[7] and agree moderately with those of Kavanagh.[8] However, the present work disagrees with the work of Baggett and Bame.[6]

III. ^{6}Li(^{3}He,n)^{8}B

The threshold energy for this reaction is E_d = 2.966 MeV. Boron-8, which decays with a half-life of about 0.75 sec, is the mirror nucleus of ^{8}Li. The positron decay proceeds mainly to the 2.90-MeV level in ^{8}Be, with a 7% branch to the 16.63-MeV level. Both of these states are α unstable.

Two groups[15, 16] have detected the ^{8}B positron activity to measure this cross section. Another group[17] used neutron time-of-flight techniques. Farmer and Class[15] report the cross section at 5.5 MeV, and it is a factor of 3 smaller than that reported by van der Merwe, McMurray, and Van Heerden[17] at the same energy. The results reported by Marrs, Bodansky and Adelberger[16] are at ^{3}He energies above 8 MeV and do not overlap the work of the other groups.

The ^{6}Li(^{3}He, n)^{8}B reaction cross section was measured at closely spaced intervals of bombarding energies between threshold and 3.8 MeV. Data were also taken at four ^{3}He energies between 5.5 and 7.6 MeV. The experimental technique used was

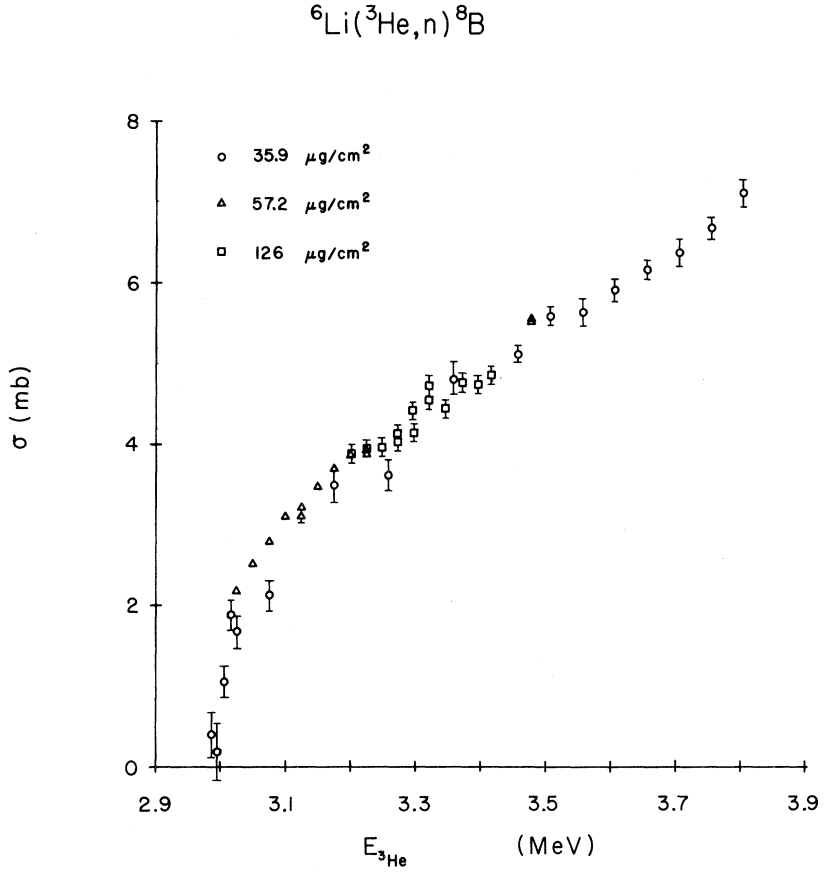

FIG. 5. Total cross section versus energy for the ^{6}Li(^{3}He, n)^{8}B reaction from threshold to 4 MeV.

essentially the same as was used to measure electrons from the decay of ^{8}Li produced by the ^{7}Li-$(d,p)^{8}$Li reaction. A 5-cm diam by 2.5-cm thick stilbene crystal detected the positrons from the ^{8}B decay. The spectra from the ^{8}B positron decay were similar to that from the ^{8}Li negatron decay, and they were processed in a similar manner.

Data were taken from threshold to 3.8 MeV using ^{3}He particles accelerated by the Dynamitron, and from 5.5 to 7.8 MeV using the beam from the tandem Van de Graaff. For these latter data a 46-cm diam scattering chamber was used that was similar in design to the 76-cm diam chamber described above. For the runs at the tandem, targets about 300 μg/cm^2 thick were evaporated onto aluminum backings that were just thick enough to stop the ^{8}B recoils. With these targets the chief backgrounds were from ^{27}Si and ^{29}P produced in the aluminum backings.

The cross sections near threshold are shown in Fig. 5, and the entire region, as well as data from other workers, is shown in Fig. 6. The present data agree with that reported by Farmer and Class,[15] and it is consistent with the data of Marrs *et al.*[16] However, the cross section reported by van der Merwe *et al.*[17] at 5.6 MeV is a factor of 3 higher than the present work.

IV. ^{6}Li$(d,\alpha)^{4}$He

This reaction has a Q of 22.4 MeV. Since the reaction products are identical particles, the angular distribution is symmetric about 90° in the center of mass. The reaction has been extensively studied,[18-23] and there is considerable disagreement in the reported absolute cross-section measurements.[20-23]

Yield and angular-distribution measurements were carried out in the 76-cm chamber. Angular distributions were taken at 13 bombarding energies spaced at approximately 250-keV intervals between 0.4 and 3.5 MeV. The angles at which differential cross sections were measured were as small as 15° and as large as 170°. Metal targets of ^{6}Li were used. Silicon surface barrier detectors measured the charged-particle spectrum. Figure 7 shows a charged-particle spectrum where it can be seen that there is virtually no background near the charged-particle peaks of interest.

A pulser peak was inserted into the spectrum in order to correct for dead time. Dead time was about 2% for most of the data, but at some forward angles it was as much as 10%.

Figure 8 shows three of the angular distributions. A Legendre polynomial fit containing the even terms up through P_4 was made to the data. Total cross sections for this reaction are shown in Fig. 9, along with the data reported in Refs. 20–23. The present data agree with the data reported by Meyer, Pheifer, and Staub,[23] but it disagrees with that reported by Bruno *et al.*[21] and by Jeronymo *et al.*[22] The present data do agree with the angular distributions and the shape of the cross section curve reported by Jeronymo *et al.*

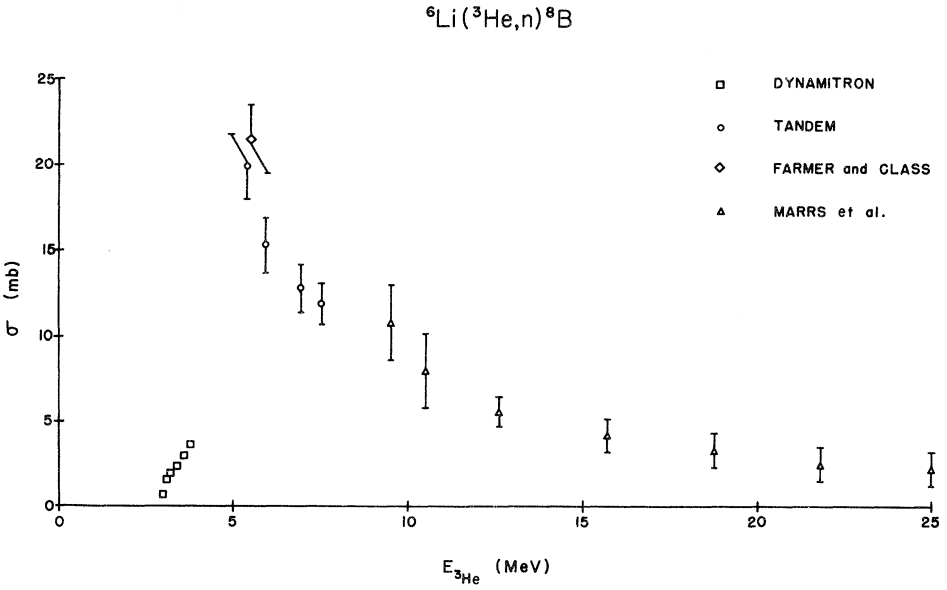

FIG. 6. Total cross section versus energy for the ^{6}Li(^{3}He, n)^{8}B reaction. The data reported in Refs. 14 and 15 are also shown.

V. ^{6}Li$(d,p)^7$Li

For this reaction, $Q = 5.0$ MeV. Lithium-7 has two bound states: the ground state and the first excited state ($E_x = 0.477$ MeV). The excited state is a $\frac{1}{2}^-$ state; therefore, the γ decay of this state is isotropic.

Most of the previous work done on this reaction has not led to absolute, total cross sections. For example, Meyer *et al.*[23] measured absolute differential cross sections at angles forward of 60°, and Birk *et al.*[24] measured relative differential cross sections at angles covering both hemispheres. The purpose of the work performed by Birk *et al.* was to determine the ratio of the total cross sections for the (d,p_0) and (d,p_1) reactions. Bruno *et al.*[21] measured total cross sections for both the (d,p_0) and (d,p_1) reactions at deuteron energies of 1.0, 1.5, and 2.0 MeV. Rickards[25] reported the cross sections for both reactions at a bombarding energy of 1.5 MeV. The data of Rickards and of Bruno *et al.* agree at 1.5 MeV, and their ratio of (d,p_0) to (d,p_1) agrees with that reported by Birk *et al.* However, at 2.0 MeV the ratio of the (d,p_0) to the (d,p_1) reaction cross sections reported by Bruno *et al.* does not agree with the ratio reported by Birk *et al.* The present measurement was carried out simultaneously with the (d,α) reaction study described above and was therefore made at the same energies and angles.

Legendre polynomial fits to the angular distributions were performed and from these total cross sections were extracted. Three angular distributions and fits for both the (d,p_0) and (d,p_1) reactions are shown in Fig. 10. The polynomial fits contained all of the Legendre polynomials of order less than or equal to a maximum order n. For all of the data taken at bombarding energies above 1.5 MeV, $n = 7$ gave a satisfactory fit. If 0.8 MeV $< E_d <$ 1.3 MeV, $n = 5$ produced a satisfactory fit. All the data with bombarding energies less than 0.8 MeV were fitted with $n = 3$. While the Legendre polynomial fits serve to parametrize the data and make convenient the extraction of total cross sections, it is not implied that the (d,p) reaction proceeds entirely through the compound nucleus. In fact, the pronounced forward peak indicates that

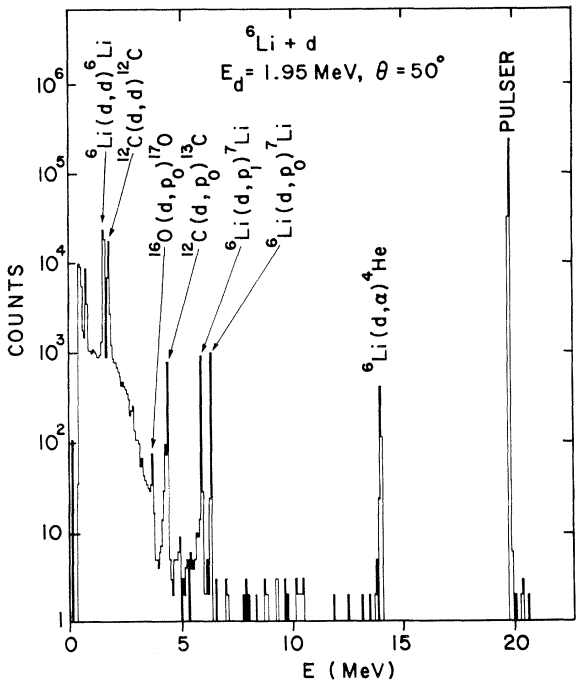

FIG. 7. Spectrum taken by a silicon surface-barrier detector during deuteron bombardment of ^{6}Li.

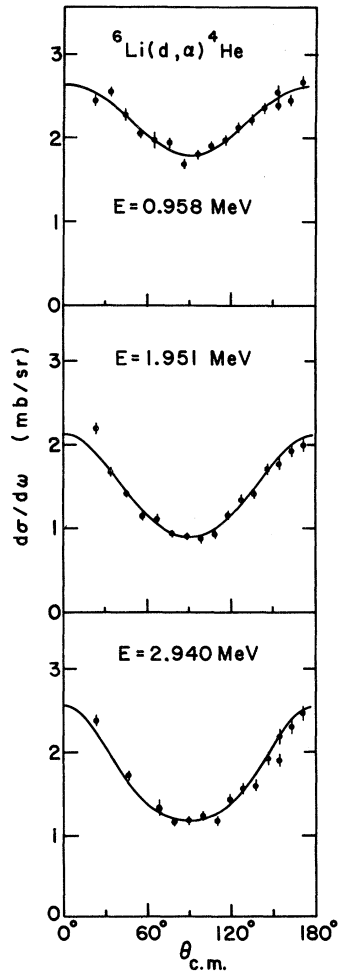

FIG. 8. Angular distributions and Legendre polynomial fits for the ^{6}Li$(d,\alpha)^4$He reaction. The fits include even terms of order less than or equal to 4.

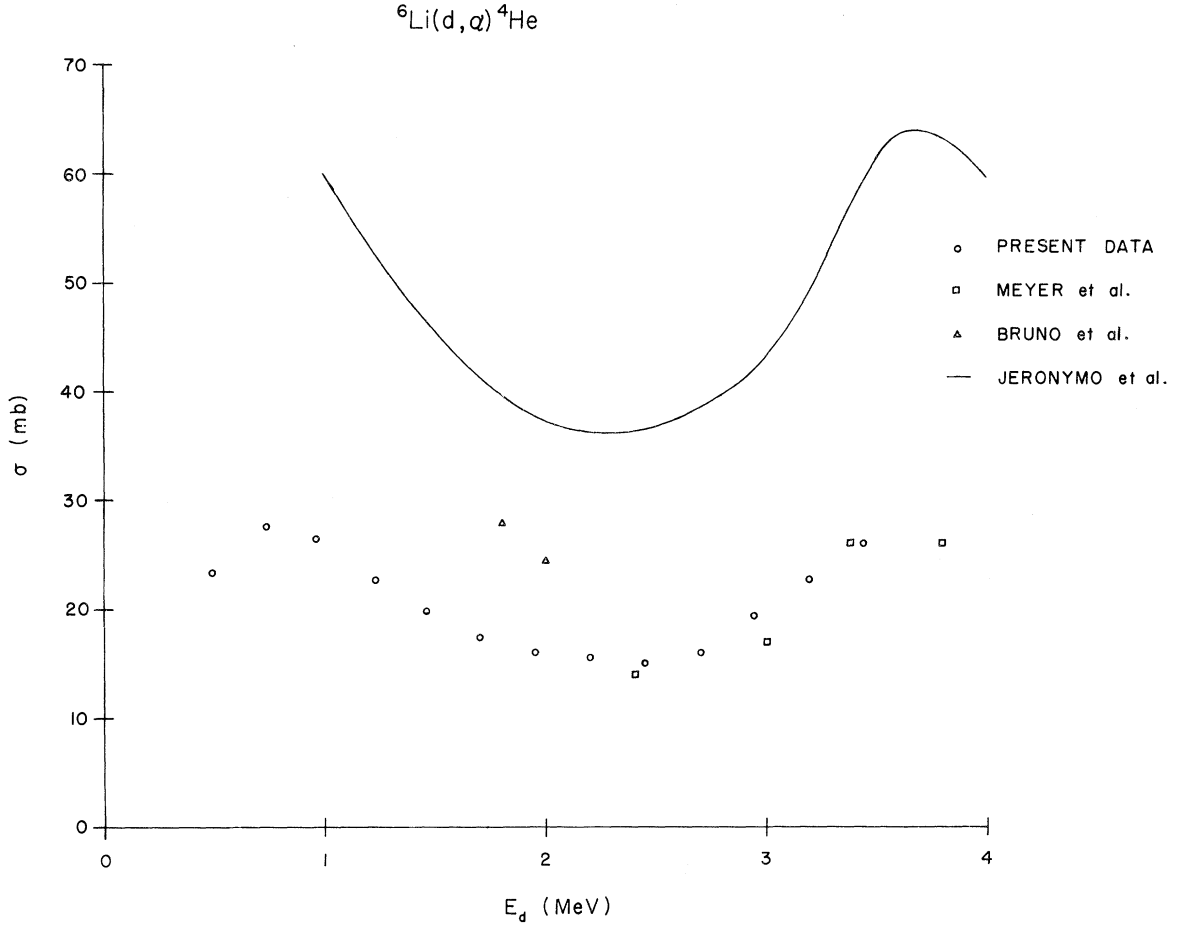

FIG. 9. Total reaction cross section as a function of energy for the ^{6}Li$(d,\alpha)^4$He reaction. The data reported in Refs. 21–23 are also shown.

TABLE II. DWBA calculation for the ^{6}Li$(d,p)^7$Li reaction cross section as a function of cutoff radius. The spectroscopic factor is assumed to be 1. The optical-model parameters were taken from Refs. 12 and 13.

^{6}Li$(d,p_0)^7$Li		E_d =1.95 MeV	
R_{co} (fm)	θ_{peak} (deg)	$\frac{d\sigma}{d\Omega}\|_{peak}$ (mb/sr)	σ (mb)
0	0	9.75	57.6
1	0	9.27	54.9
2	0	5.88	37.1
3	16	2.71	16.6
3.2	24	2.50	12.9
3.4	28	2.66	12.4
3.6	32	2.73	12.4
3.8	32	3.01	13.0
4	32	3.26	13.8
5	36	3.53	14.7
6	36	2.51	9.97
7	32	1.46	5.25

direct interactions play a significant role.

Since stripping is apparently significant in the ^{6}Li$(d,p)^7$Li reaction at energies below 3.5 MeV, DWBA calculations were performed for these data. The code DWUCK[11] was used, and the optical-model parameters were taken from Refs. 12 and 13. The spectroscopic factor for (d,p) reactions is defined in the DWUCK instructions[11] to be

$$S=\frac{d\sigma/d\Omega\,|_{exp}}{d\sigma/d\Omega\,|_{DW}}\,\frac{2(2J_i+1)(2J+1)}{1.53(2J_f+1)(2s+1)}\,, \tag{1}$$

where $d\sigma/d\Omega$ is the differential cross section, J is the angular momentum of the orbit into which the particle is transferred, J_i and J_f are the initial and final state angular momenta, and s is the spin of the transferred particle. In contrast to the ^{7}Li(d,p) reaction, for the ^{6}Li(d,p) it was found that the inner cutoff radius had a pronounced effect on the shape of the calculated angular distributions. With a cutoff radius of 3 fm or less, the angular

distributions had a pronounced backward peak that was comparable in height to the forward peak. If the cutoff radius was 4 fm or larger, the backward peak was virtually gone. Figure 11 shows the data for the (d,p_0) reaction at $E_d = 1.95$ MeV and six DWBA calculations that were performed with cutoff radii between 3.0 and 4.0 fm. The DWBA calculation was normalized to the data at angles of less than 60°.

Table II lists the calculated position, height of the peak, and the total cross section for a number of cutoff radii for the (d,p_0) reaction at 1.95 MeV, assuming that the spectroscopic factor $S=1$. A value of 3.8 fm was chosen for the cutoff radius, because it best fit the position of the peak. Clearly, the spectroscopic factor is sensitive to the cutoff radius and, therefore cannot be determined accurately from data taken at these low bombarding energies.

A curve consisting of an incoherent sum of an isotopic compound nuclear contribution and the DWBA calculation were fit to the data. The spectroscopic factor was extracted from the fit, and it ranged from about 1 to 2. The resulting curves fit the data only in its general features (see Fig. 12). The spectroscopic factor could have been reduced by decreasing the cutoff radius. However, then the first maximum would have been at the wrong angle. Perhaps a more detailed DWBA analysis involving varying the optical-model parameters would have produced a better fit to the data. However, it was felt that little new physics could be learned from such manipulations, and therefore this line was not pursued.

Schiffer *et al.*[26] measured the (d,p_0) and (d,p_1) reaction cross sections at 12 MeV and found spectroscopic factors of 0.90 and 1.15, respectively, in fair agreement with the values of 0.721 and 0.893 predicted by Cohen and Kurath.[27] Powell *et al.*[28] performed DWBA and Hauser-Feshbach calculations for this reaction at 5 MeV, and found

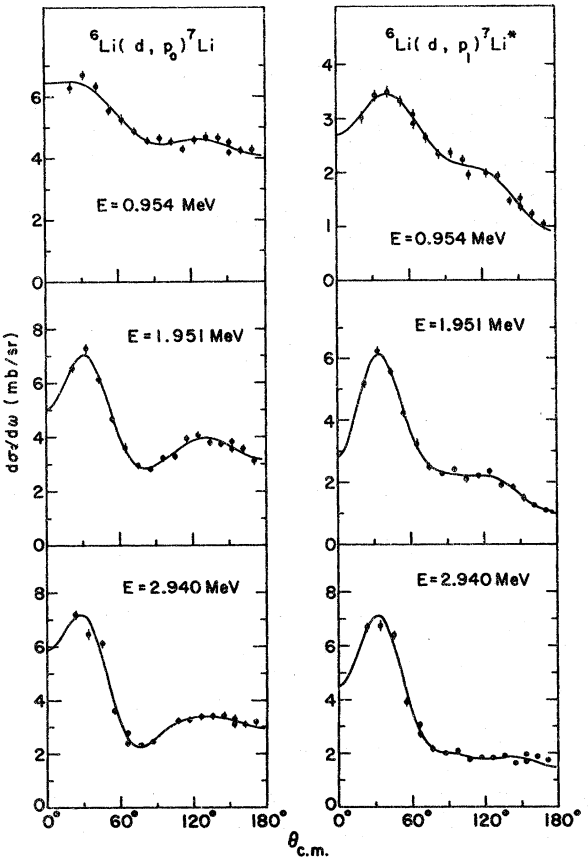

FIG. 10. Angular distributions and Legendre polynomial fits for the ^{6}Li$(d,p)^7$Li reaction. P_7 is the highest order polynomial used in the fits.

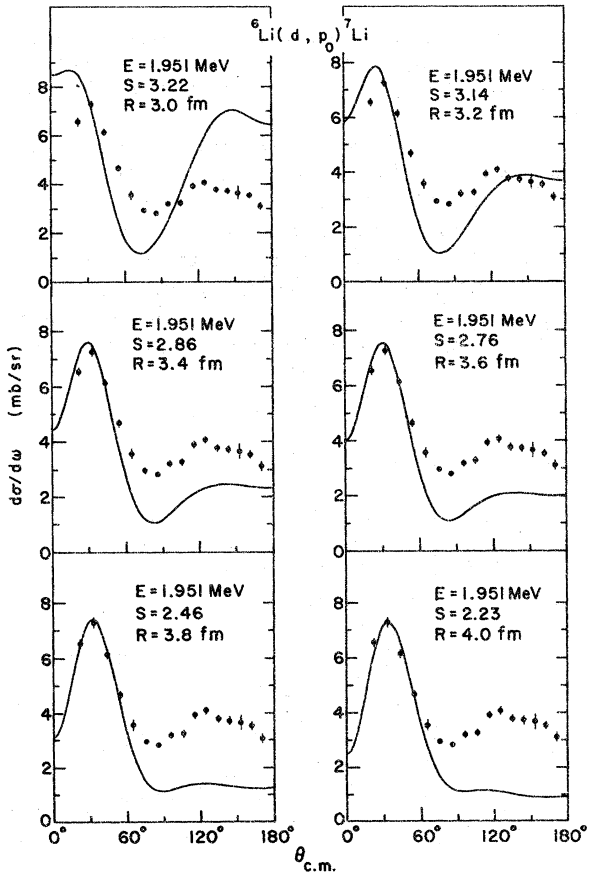

FIG. 11. The ^{6}Li$(d,p_0)^7$Li data taken at $E_d = 1.95$ MeV and six DWBA calculations that were performed with cutoff radii between 3.0 and 4.0 fm. The calculations were normalized to the data at angles forward of 60°. S is the spectroscopic factor (defined in the text) and R is the inner cutoff radius of the DWBA calculation.

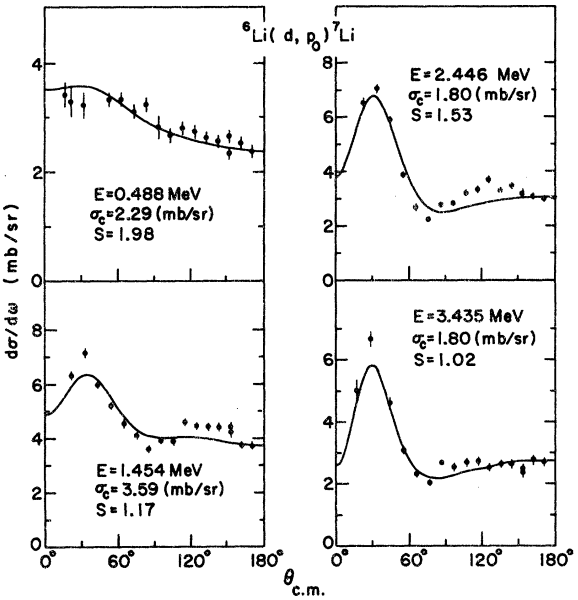

FIG. 12. A DWBA calculation plus an isotropic term fit to the ^{6}Li(d, p)^{7}Li angular distributions. σ_c is the isotropic intensity, and S is the spectroscopic factor.

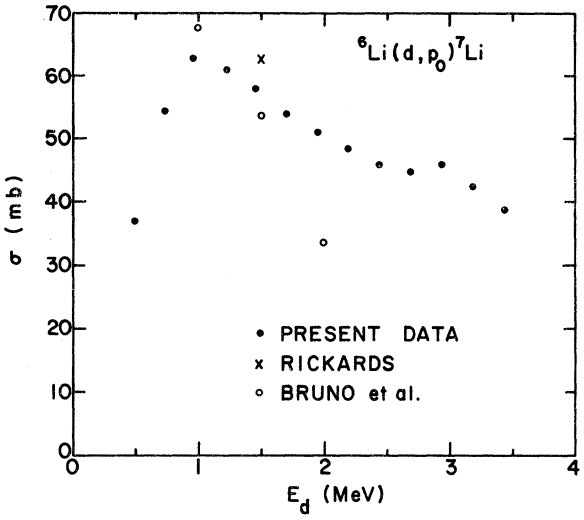

FIG. 14. Total cross section for the ^{6}Li(d, p)^{7}Li reaction. The data reported in Refs. 21 and 25 are also shown.

that an incoherent sum of these two calculations gave a good fit to the differential cross-section data at this energy.

In addition to observing the charged-particle spectra, the γ rays from the decay of the first excited state of ^{7}Li were detected through a 1-cm Lucite window, located at an angle of 80° relative to the beam by a Ge(Li) detector. The efficiency of the γ-ray detector was measured by placing calibrated ^{133}Ba and ^{137}Cs sources at the target's position. Dead time corrections in the calibration of between 2 and 6% were made by introducing a pulser peak into the spectrum. Uncertainty in the detector efficiency is estimated to be 5%. A spectrum taken by the Ge(Li) detector is shown in Fig. 13.

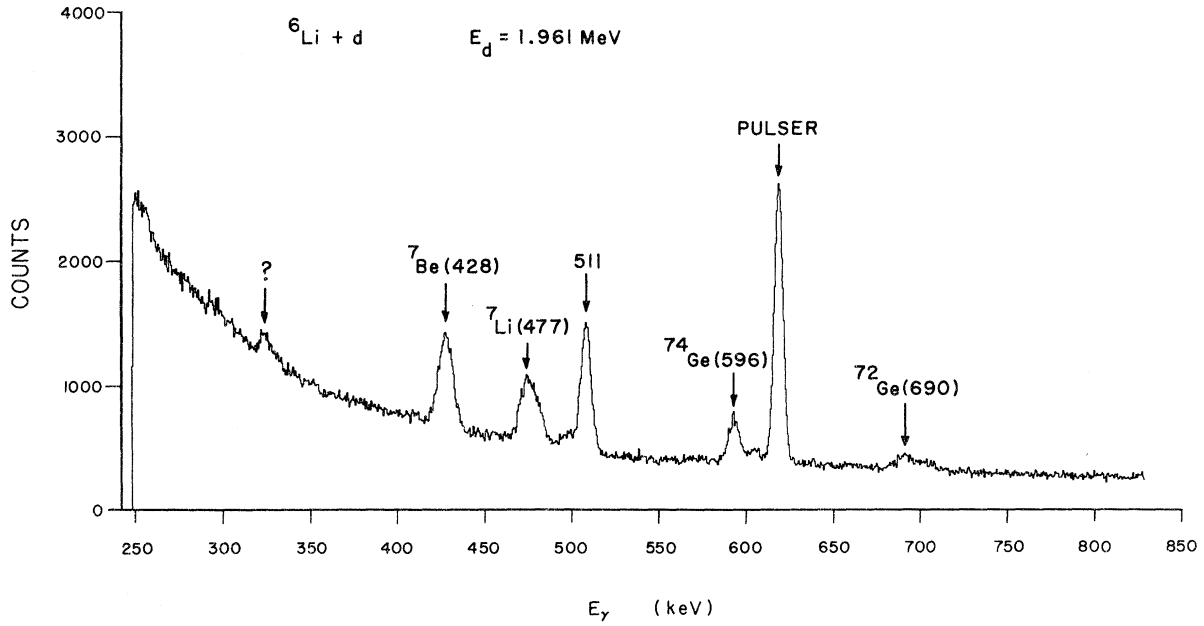

FIG. 13. γ-ray spectrum taken by a Ge(Li) detector during deuteron bombardment of ^{6}Li.

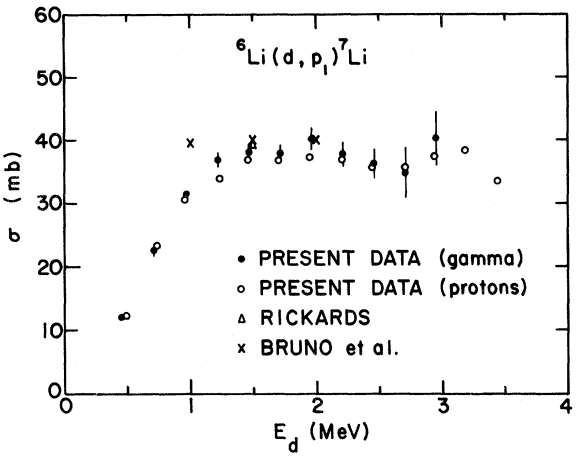

FIG. 15. The total cross section for the ^{6}Li$(d, p_1)^7$Li* reaction. The data reported in Refs. 21 and 25 are also shown.

The total cross sections found here for the ^{6}Li$(d,p)^7$Li reactions are shown in Figs. 14 and 15. γ-ray and proton-yield measurements of the (d,p_1) reaction cross section agree quite well. Error bars represent the stistical uncertainty of the points. Where no error bar is shown, the statistical uncertainty is comparable to or smaller than the size of the point.

The present data agree with the (d,p) data reported by Rickards,[25] but do not agree well with that reported by Bruno *et al.*[21] In particular, Bruno *et al.* indicate that at 2 MeV the (d,p_0) reaction cross section is less than the (d,p_1) reaction cross section. The present results do not support this; moreover, Birk *et al.*[24] report that at bombarding energies below 3.3 MeV the (d,p_0) reaction cross section is always larger than the (d,p_1) reaction cross section. The (d,p_0) to (d,p_1) reaction cross-section ratios for the presently reported data agree well with the ratios reported by Birk *et al.*[24]

VI. ^{6}Li$(d,n)^7$Be

This is the mirror reaction of ^{6}Li$(d,p)^7$Li. Beryllium-7 also has only two bound states, and the excited state is again a $\frac{1}{2}^-$ level. As a result, the γ decay of the excited state in ^{7}Be is also isotropic. The (d,n) reaction has a ground-state Q of 3.4 MeV. Because of charge symmetry, one would expect the ratio of the (d,p_0) to the (d,p_1) reaction cross sections to be similar to the ratio of the (d,n_0) to the (d,n_1) reaction cross sections. This has been shown experimentally to be true over the energy range 0.4–3.3 MeV[24,29] to an accuracy varying from 3% at 3 MeV to 12% at 0.5 MeV. In order to measure the (d,n_1) cross section, the γ-ray

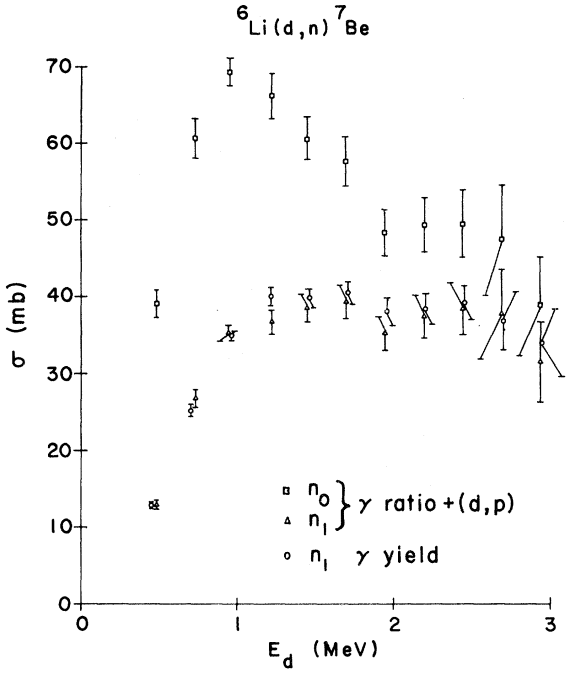

FIG. 16. The cross section versus energy for the ^{6}Li$(d,n)^7$Be reaction.

yield was measured at 11 bombarding energies spaced at approximately 250-keV intervals between 0.4 and 3.0 MeV. This was performed simultaneously with the (d,p_1) reaction described above (Fig. 13).

The (d,n_0) and (d,n_1) reaction cross sections were inferred from the (d,p) cross sections and the ratio of the 428-keV to the 477-keV γ-ray yields. Specifically,

$$\frac{\sigma(d,n_0)}{\sigma(d,n_1)} = \frac{\sigma(d,p_0)}{\sigma(d,p_1)} \tag{2}$$

or

$$\sigma(d,n_0) = \sigma(d,p_0)\frac{\sigma(d,n_1)}{\sigma(d,p_1)} = \sigma(d,p_0)\frac{\gamma_{428}}{\gamma_{477}}. \tag{3}$$

Figure 16 shows the results of the cross-section determinations for the ^{6}Li$(d,n)^7$Be reaction. The error bars represent statistical uncertainties, which include the uncertainty in determining the background. In addition to the statistical uncertainty, there is an absolute uncertainty of about 15% which has been discussed above. Agreement between the two methods of determining the (d,n_1) reaction cross section is not surprising since it is the result of the fact that the two methods of measuring the (d,p_1) reaction cross section agree well.

There are no total cross sections for the ^{6}Li$(d,n)^7$Be reaction previously reported in the literature for this energy region.

VII. CONCLUSIONS

Various checks have been made on the data reported herein with particular attention paid to target thickness and stability. As a result, it is felt that the cross sections reported here are accurate to the stated 15% uncertainty. An accuracy of 25% has been deemed sufficient for thermonuclear reactor design studies.

The reactions studied are tabulated in Table I. In each case where total cross sections are reported for one of these reactions by other groups, the present results agree with at least one of those groups, usually the one reporting the smallest cross sections.

McNally[1] has emphasized both the promise for CTR that chain reactions involving the burning of ^{6}Li holds and the paucity of the relevant nuclear reaction data. Cross sections for three of the reactions important in ^{6}Li burning have been measured in the present work. If data are needed over a greater energy range some extrapolation could be made from the present data and, if that is not adequate, further measurements would not be difficult. In addition, other reactions must be studied before sufficient data on ^{6}Li will have been acquired. In particular, accurate measurements are needed of inelastic scattering cross sections and of reactions leading to three body final states. Nevertheless, the present results represent a significant step toward satisfying the cross-section data requirements for the CTR program on reactions involving the Li isotopes.

---

*Present address: Air Force Weapons Laboratory, Kirtland Air Force Base, New Mexico 87117.

†Work supported in part by the National Science Foundation.

‡Work performed under the auspices of the U. S. Atomic Energy Commission.

[1]J. R. McNally, Jr., Nucl. Fusion 11, 187 (1971); private communication.

[2]L. Stewart, M. S. Moore, and H. T. Motz, Los Alamos Scientific Laboratory Report No. La-5253-MS, 1973 (unpublished).

[3]V. S. Crocker, S. Blow, and C. J. H. Watson, Culham Laboratory Report No. CLM-P240, 1970 (unpublished).

[4]J. R. Lemley, private communication.

[5]T. Lauritsen and F. Ajzenberg-Selove, Nucl. Phys. 78, 1 (1966).

[6]L. M. Baggett and S. J. Bame, Phys. Rev. 85, 434 (1952).

[7]S. Bashkin, Phys. Rev. 95, 1012 (1954).

[8]R. W. Kavanagh, Nucl. Phys. 15, 411 (1960).

[9]L. F. Chase, R. G. Johnson, F. J. Vaughn, and E. K. Warburton, Phys. Rev. 127, 859 (1962).

[10]J. P. F. Sellschop, Phys. Rev. 119, 251 (1960).

[11]P. D. Kunz, Instruction for the Use of DWUCK, 1969 (unpublished).

[12]G. R. Satchler, Nucl. Phys. 85, 273 (1966).

[13]B. A. Watson, P. P. Singh, and R. E. Segel, Phys. Rev. 182, 977 (1969).

[14]J. B. Woods and D. H. Wilkinson, Nucl. Phys. 61, 661 (1965).

[15]B. J. Farmer and C. M. Class, Bull. Am. Phys. Soc. 6, 341 (1961).

[16]R. E. Marrs, D. Bodansky, and E. G. Adelberger, Phys. Rev. C 1, 427 (1973).

[17]P. van der Merwe, M. R. McMurray, and I. J. van Heerden, Nucl. Phys. A103, 474 (1967).

[18]N. P. Heydenburg, C. M. Hudson, D. R. Inglis, and W. D. Whitehead, Phys. Rev. 74, 405 (1948).

[19]G. S. Mani, R. M. Freeman, F. Picard, D. Redon, and A. Sadeghi, Proc. Phys. Soc. 85, 281 (1965).

[20]Y. P. Antoufiev, M. M. El-Shesheni, H. R. Saad, Z. A. Saleh, and P. V. Sorokin, Nucl. Phys. 48, 299 (1963).

[21]G. Bruno, J. Decharge, A. Perrin, G. Surget, and C. Thibault, J. Phys. (N.Y.) 27, 517 (1966).

[22]J. M. F. Jeronymo, G. S. Mani, F. Picard, and A. Sadeghi, Nucl. Phys. 38, 11 (1962).

[23]V. Meyer, W. Pfeifer, and H. H. Staub, Helv. Phys. Acta. 36, 465 (1963).

[24]M. Birk, G. Goldring, P. Hillman, and R. Moreh, Nucl. Phys. 41, 58 (1963).

[25]J. Rickards, Rev. Mex. Fis. 14, 241 (1965).

[26]J. P. Schiffer, G. C. Morrison, R. H. Siemssen, and B. Zeidman, Phys. Rev. 164, 1274 (1967).

[27]S. Cohen and D. Kurath, Nucl. Phys. A101, 1 (1967).

[28]D. L. Powell, G. M. Crawley, B. V. N. Rao, and B. A. Robson, Nucl. Phys. A147, 65 (1970).

[29]L. Cranberg, A. Jacquot, and H. Liskien, Nucl. Phys. 42, 608 (1963).